High-Power Coherent Microwave Emission from Magnetic Tunnel Junction Nano-oscillators with Perpendicular Anisotropy

Zhongming Zeng,[†,×,*] Pedram Khalili Amiri,[‡] Ilya N. Krivorotov,[§] Hui Zhao,[⊥] Giovanni Finocchio,[¶] Jian-Ping Wang,[⊥] Jordan A. Katine,[#] Yiming Huai,[▽] Juergen Langer,[○] Kosmas Galatsis,[‡] Kang L. Wang,[‡] and HongWen Jiang[†]

[†]Department of Physics and Astronomy, [‡]Department of Electrical Engineering, University of California, Los Angeles, California 90095, United States, [§]Department of Physics and Astronomy, University of California, Irvine, California 92697, United States, [⊥]Department of Electrical and Computer Engineering, University of Minnesota, Minneapolis, Minnesota 55455, United States, [¶]Department of Matter Physics and Electronic Engineering, University of Messina, Messina 98166, Italy, [#]Hitachi Global Storage Technologies, San Jose, California 95135, United States, [▽]Avalanche Technology, Fremont, California 94538, United States, and [○]Singulus Technologies, Kahl am Main 63796, Germany. [×]Present address: Suzhou Institute of Nanotech and Nanobionics, Chinese Academy of Sciences, Ruoshui Road 398, 215123 Suzhou, P.R. China.

ABSTRACT The excitation of the steady-state precessions of magnetization opens a new way for nanoscale microwave oscillators by exploiting the transfer of spin angular momentum from a spin-polarized current to a ferromagnet, referred to as spin-transfer nano-oscillators (STNOs). For STNOs to be practical, however, their relatively low output power and their relatively large line width must be improved. Here we demonstrate that microwave signals with maximum measured power of 0.28 μW and simultaneously narrow line width of 25 MHz can be generated from CoFeB–MgO–based magnetic tunnel junctions having an in-plane magnetized reference layer and a free layer with strong perpendicular anisotropy. Moreover, the generation efficiency is substantially higher than previously reported STNOs. The results will be of importance for the design of nanoscale alternatives to traditional silicon oscillators used in radio frequency integrated circuits.

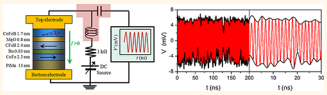

KEYWORDS: spin-transfer nano-oscillators · microwave · magnetic tunnel junction · perpendicular anisotropy · magnetoresistance

In recent years, spin-transfer nano-oscillators (STNOs) based on spin transfer torque[1,2] have attracted intense attention due to their potential applications in modern communications.[3−20] STNOs have potential advantages over transistor-based voltage controlled oscillators (VCOs), such as simple structure, smaller size, and lower cost, and are easily integrated onto silicon. However, to readily supplant VCOs in most applications, STNOs will need to deliver comparable power levels[5] and simultaneously possess a single oscillation mode with a narrow line width. The power generated in a STNO is determined by several factors. The first one is the resistance change induced by the magnetoresistance (MR) effect in the magnetization oscillations. MgO-based magnetic tunnel junctions (MTJs) with large MR ratios (>50%) can therefore deliver larger microwave signals than metallic oscillators with MR ratios lower than 10%.[12−17] The second requirement for a large emitted power is the excitation of large-amplitude magnetization oscillations. To accomplish this, one can use a nonzero offset angle between the orientation of the reference and free-layer magnetizations.[20] Furthermore, the oscillation amplitude and the resulting power increase with I/I_c, where I is the bias current and I_c is the critical current for the onset of spin-transfer-torque (STT) induced microwave emission.[21] However, in MTJ STNOs the maximum bias current is limited by the barrier breakdown voltage (~1 V). In many cases this does not allow for the application of sufficiently large bias currents needed to induce large-amplitude oscillations. Moreover, at large bias currents, the MR ratio decreases due to spin excitations localized at the interfaces between the magnetic electrodes and the tunnel barrier.[22] The solution is thus to reduce I_c without increasing I in order to achieve large-amplitude precession by increasing I/I_c. The I_c value of an in-plane magnetized MTJ can be reduced by increasing the perpendicular anisotropy of the free layer.[23−26] The critical current density J_c for current-induced

* Address correspondence to zhongming.zeng@gmail.com.

Received for review March 20, 2012 and accepted June 4, 2012.

Published online June 04, 2012
10.1021/nn301222v

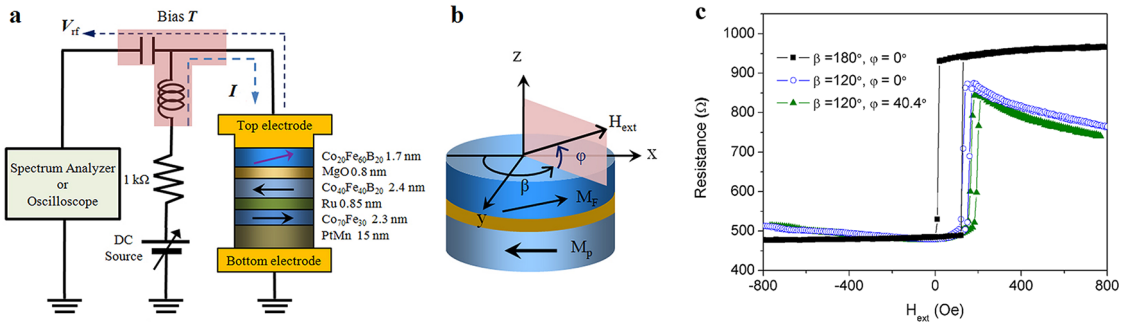

Figure 1. (a) Measurement principle and sign convention for current. Positive current flowing from the free to the reference layer favors the parallel state. Oscillatory voltage generated by spin-transfer-torque is monitored directly on a spectrum analyzer or real-time oscilloscope without amplifier. (b) Definition of the coordinate system. Here β is the angle between the external magnetic field H_{ext} and the reference layer in the $x-y$ plane, and φ is the angle with respect to the $x-y$ plane. The positive H_{ext} (*i.e.*, positive in-plane field component) favors the antiparallel state. The precession axis may be misaligned from the external field direction. (c) Resistance as a function of magnetic field for different field directions.

magnetic excitation is derived from the instability condition of the easy plane component of magnetization given by[23] $J_c \approx (2e\alpha M_s t/(\hbar\eta))(H_k + (H_d - H_{k\perp})/2)$, where α is the damping constant, η is the spin-transfer efficiency, M_s and t are the free layer saturation magnetization and thickness, H_k is the in-plane shape-induced anisotropy, $H_d \approx 4\pi M_s \gg H_k$ is the demagnetizing field, and $H_{k\perp}$ is the free layer perpendicular anisotropy. Increasing $H_{k\perp}$ can reduce J_c (hence I_c) by partially canceling the effect of the demagnetizing field H_d. However, so far there have been no reports of magnetization oscillations in a system with strong perpendicular anisotropy that simultaneously provides high MR ratio. Here we demonstrate that CoFeB−MgO MTJs containing an in-plane magnetized reference layer and a free layer with strong perpendicular anisotropy are excellent candidates for high-power and narrow line width STNO applications. This configuration differs from that reported recently for magnetization switching,[27] where both the reference and the free layers are out-of-plane magnetized. It does benefit from the use of the CoFeB−MgO system, however, which is the most widely used MTJ material combination for memory applications. Due to the partial cancellation of the out-of-plane demagnetizing field by the perpendicular anisotropy, this system offers an additional advantage, in that it allows one to investigate the dynamics of the free layer in changing applied field orientation without the need to apply large out-of-plane fields, hence keeping the orientation of the reference layer essentially constant.

RESULTS AND DISCUSSION

A schematic of our experiment is shown in Figure 1a. The STNO devices are ellipse-shaped pillars formed by the $Co_{70}Fe_{30}$/Ru/$Co_{40}Fe_{40}B_{20}$ in-plane magnetized reference layer, MgO insulator, and the $Co_{20}Fe_{60}B_{20}$ in-plane magnetized free layer with perpendicular anisotropy. The devices in this study have nominal dimensions of 170 nm × 60 nm and a free layer thickness of 1.7 nm, which remains in-plane magnetized in zero external field while providing a significant compensation of the demagnetizing field by the perpendicular anisotropy.[26] The positive current I flowing from the free layer to the reference layer favors the parallel (P) state (Figure 1a). The typical MR transfer curves as a function of external field are shown in Figure 1c for different field orientations (illustrated in Figure 1b), for a low bias current of I = 10 μA. The MR and the resistance-area (RA) product in the parallel state are 102% and 3.8 Ω μm^2, respectively. A small loop shift is observed, which is due to the coupling between free and reference layers.

The oscillation characteristics of STNOs are determined from the microwave signals generated due to the MR effect.[3] This oscillatory output is directly detected using a 26 GHz spectrum analyzer, or a high speed real time oscilloscope with 6 GHz bandwidth and 20 G samples/s rate without amplifier as shown in Figure 1a. The measurements were carried out at room temperature for various field orientations. We observe coherent microwave signals with high power and narrow line width when the external field is applied at β = 120°. The plots of the power spectral density (Figure 2a,b) illustrate their dependence on the bias current I for two different field orientations: in-plane field (β = 120° and φ = 0°) and out-of-plane field (β = 120° and φ = 40.4°). Here, a positive (in reference to the in-plane field component as shown in Figure 1b) field stabilizes the antiparallel (AP) state while a positive current favors the P state, thus the spin torque counteracts the damping and can bring the magnetization of the free layer into a stable precession. In both cases the microwave signals show a qualitatively similar current dependence. For I = 0.1 mA, no obvious microwave signals are observed due to the low power (no amplification is performed in the measurement). When 0.2 mA ≤ I < 0.4 mA, we observe one evident oscillation peak along with low frequency noise, suggesting an incoherent magnetization precession.[19] Above 0.4 mA,

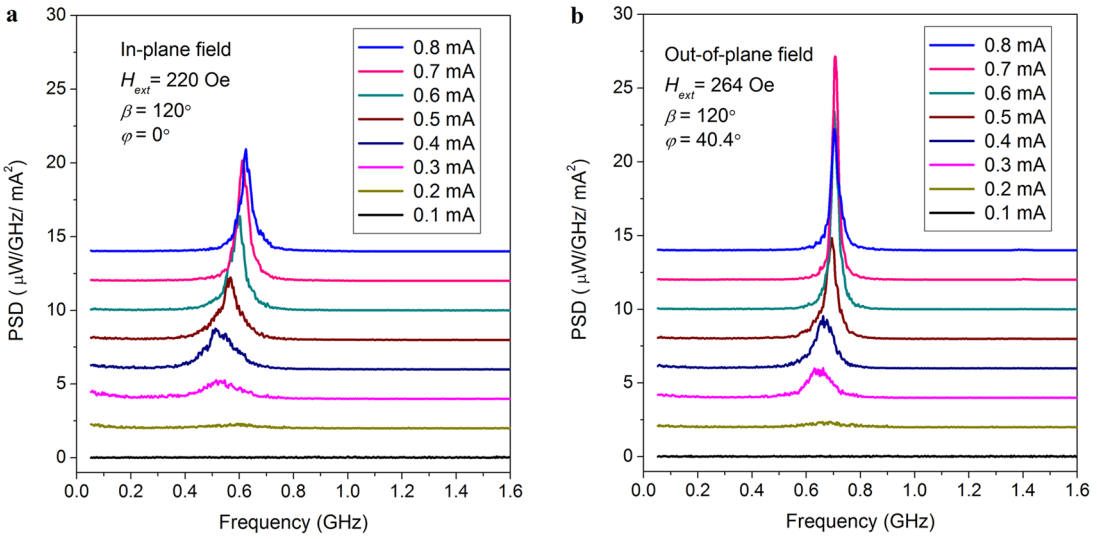

Figure 2. Microwave emission spectra measured at positive currents between 0.1 mA and 0.8 mA with 0.1 mA steps. The power spectral densities (PSD) normalized by I^2 have been offset by 2 μW/GHz/mA^2 for clarity. (a) Microwave signals measured for the in-plane field, *i.e.*, β =120° and φ = 0°. (b) Spectra for the out-of-plane field, *i.e.*, β =120° and φ = 40.4°.

the low frequency noise is largely suppressed and only one oscillation peak is present, giving a clear indication of the steady-state magnetization precession. As the current amplitude is further increased to I = 0.8 mA, the dynamics are characterized by an obviously broader line width. The oscillation frequencies of the microwave signals are shown in Figure 3a as a function of applied current for both in-plane and out-of-plane fields. One can notice that the oscillation frequencies for all currents are in the sub-GHz range (comparable to that of vortex oscillators, arising from the coherent gyrotropic motion of the magnetic vortex core[9]), which is a consequence of the significant compensation of the demagnetizing field $\mathbf{H}_d$ by the strong perpendicular anisotropy. By comparison, in previously reported MTJ STNO experiments,[12−19] the oscillation frequencies were usually in the range of several GHz because of the large demagnetizing field $\mathbf{H}_d$ (~10 kOe) and the absence of the perpendicular anisotropy. It can be also seen that the frequency decreases with increasing dc current in the low-current regime, while it increases with current in the high-current regime, suggesting that the steady-state excitation corresponds to an in-plane precession (IPP) mode only for small currents.

Figure 3 panels b and c show the measured power and line width of microwave signals as a function of current for the in-plane and out-of-plane fields. The measured power rapidly increases while the line width decreases significantly when the current is increased from 0.2 to 0.7 mA. The optimal condition exhibiting both large power and narrow line width occurs at I = 0.7 mA, corresponding to a current density of J = 8.7 MA/cm^2. At this current, for the in-plane field case the power reaches up to 0.26 μW together with a line width of 47 MHz, while for the out-of-plane field case the microwave signal has a power of 0.28 μW and a narrow line width of 25 MHz. Note that the powers presented here are data measured directly by the spectrum analyzer, and therefore suffer from the effect of impedance mismatch with the 50 Ω system impedance. The maximum output power that can be delivered to a matched load is in fact >0.95 μW (Supporting Information, Note 1). This is, to the best of our knowledge, the highest output power for STNOs reported to date. Most importantly, these oscillators have a simultaneously narrow line width comparable to those obtained in low-MR MTJ STNOs,[12,13,18,19] along with suppression of the secondary oscillation modes. By comparison, previously reported STNOs either exhibited large power with large line width[13−16] and multiple modes[13−15] or low power together with narrow line width.[18,19] In addition, the generation efficiency $\varepsilon = P_{exp}/P_{input}$ of our oscillators is substantially higher compared to other STNOs ($\varepsilon \sim$ 0.01%,[14] 0.02%[17]). Here, P_{exp} is the output power, $P_{input} = I \times V$ is the input power and V is the dc voltage applied to the device. The output power P_{exp} is 0.28 μW at I = 0.7 mA and V = 401 mV, yielding $\varepsilon \sim$ 0.1% (>0.34% if impedance matched) for this work. These microwave emissions with large power, narrow line width, single oscillation mode, and improved generation efficiency at low current are substantially closer to those required for practical applications. We note that, the line width becomes further narrower by continuing to increase the out-of-plane angle of the field. At φ = 57°, for example, the line width is about 16 MHz, but power is also reduced due to the decrease in resistance change and oscillation amplitude (Supporting Information, Figure S1).

To identify the amplitude of oscillations in the STNOs presented here, we extract the dynamic resistance variation ΔR_{dyn} from the measured power spectral densities[10] for both in-plane and out-of-plane fields,

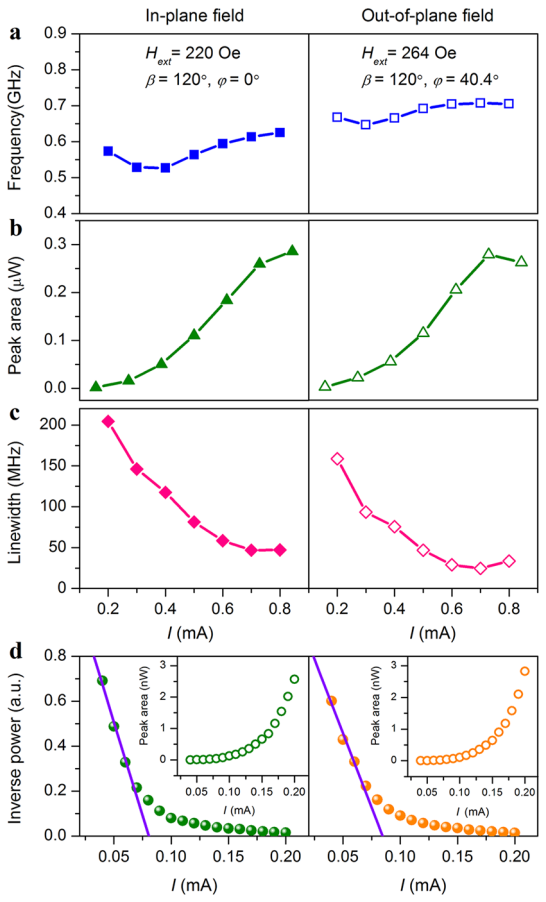

Figure 3. Current-induced precession: current dependences of peak frequency, power, and line width, as well as critical currents of the microwave emissions. Left panels, in-plane field; and right panels, out-of-plane field. The data in panels a–c have been extracted from the spectra in Figure 2: (a) Current dependence of peak frequency; (b) the width of the peak as a function of the current; (c) integrated power as a function of the current; (d) dependence of the inverse normalized power $(P_{exp}/I^2)^{-1}$ on the current (dots, experiment; solid line, theoretical fit[21]). Insets in panel d show the integrated power in near-onset range of currents obtained by amplifying with a 10 dB amplifier.

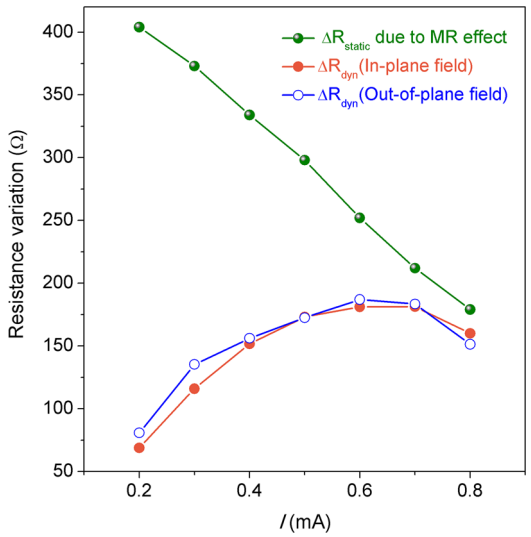

Figure 4. Current dependence of ΔR_{static} (olive) resulting from MR effect. Orange circles represent in-plane field ΔR_{dyn} and blue open circles represent out-of-plane field ΔR_{dyn}.

which are shown in Figure 4 as a function of current. Three main features can be identified as follows. First, the ΔR_{dyn} values are larger than 100 Ω for $I > 0.3$ mA, resulting in large output microwave signals. Second, ΔR_{dyn} increases with increasing current, reaches a maximum at $I = 0.6$ mA, and remains constant up to $I = 0.7$ mA, where ΔR_{dyn} corresponds to approximately 85% of the total static resistance change ΔR_{static} due to the MR effect, suggesting a very large amplitude precession. Third, as the current is increased past the optimum, ΔR_{dyn} decreases due to the reduction in the MR ratio. The reason for the observed large-amplitude oscillation is the small I_c value, which is determined to be less than 0.1 mA by identifying deviations from a linear dependence for the *inverse* power on the bias current for small values of current, *i.e.*, $(P_{exp}/I^2)^{-1} \propto (I_c - I)$[21] (Figure 3d). The small I_c allows sufficiently large currents to be applied safely to the samples, leading to I/I_c values of larger than 8 in this study, compared to less than ~3 due to the larger I_c values in most MTJ STNOs reported so far.[12–19] Thus, the contribution of the perpendicular anisotropy in the planar free layer allows us to realize the large-amplitude oscillations by achieving a large I/I_c at low bias current I, which is consistent with the results of our micromagnetic simulations (Supporting Information, Note 5)

We now discuss the possible mechanisms responsible for the observed narrow line width in the system presented here. First, we believe that this is associated with the improved uniformity of the magnetization oscillations. As mentioned above, the free layer has a relatively large perpendicular anisotropy field, which is still smaller than the demagnetizing field; thus, the free layer exhibits in-plane magnetization. The effect of the perpendicular anisotropy on STT precession is qualitatively similar to that of a magnetic field applied perpendicular to the plane of STNOs in the experiment,[28] which leads to a uniform demagnetizing field in the nanosized pillars. A result of this is that only one oscillation mode is present in our STNOs for all currents, while previous works[13–15] have reported multiple oscillation modes. This is further verified by tilting the field orientation out of plane. The dynamics become more uniform while maintaining the same oscillation amplitude in the out-of-plane field case compared to the in-plane field case (Figure 5a,b, or Supporting Information, Figure S3), resulting in line width narrowing (Figure 3c). Second, in the STT-induced microwave regime, the line width decreases with oscillation energy E or amplitude A.[29] Our data offer strong evidence that the oscillation amplitude plays an important role in determining the line width

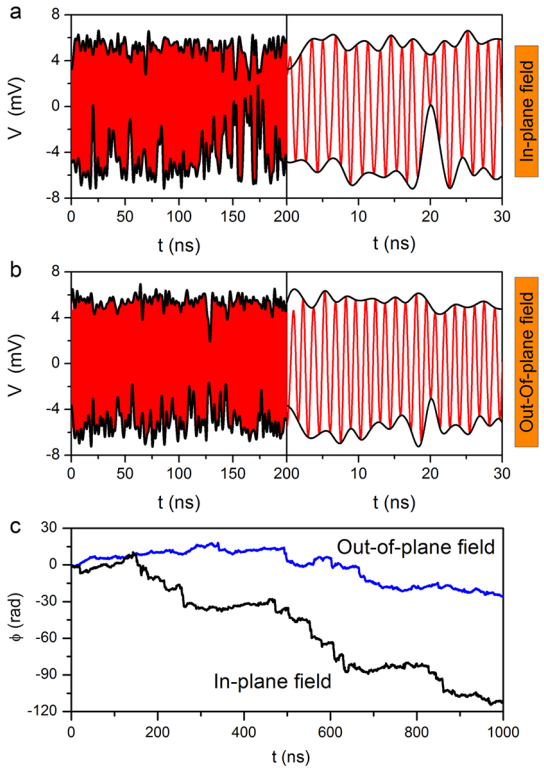

Figure 5. Time-resolved voltage traces and phase deviations. Time-resolved voltage traces are recorded by a single-shot oscilloscope triggered by the signal itself. Left panels in panels a and b show 200 ns segments of the full time (1 μs) traces at I = 0.7 mA for the in-plane field (β =120° and φ = 0°) and the out-of-plane field (β = 120° and φ = 40.4°), respectively. The signal is shown in red, and the positive and negative envelopes are in black. Right panels in panels a and b are 30 ns window zooms of the previous traces. (c) Phase deviations (for the corresponding definition see refs 31 and 32,) for 1 μs time-traces. Note that we numerically applied a 600 MHz band-pass filter centered at peak frequency to eliminate the background noise, low frequency noise, and related harmonics.

(see Figure 4 or Supporting Information, Figure S3). In the low-current regime (0.2 ≤ I < 0.4 mA), the precession amplitude is small, that is, ∼ 3.0 mV (peak-to-peak). This small-amplitude motion of the magnetization produces relatively large linewidths (Figure 3c) due to the enhanced relative effect of thermal fluctuations for small-amplitude magnetization oscillations.[21,30] In the large-amplitude precession regime (I ≥ 0.4 mA), the precession amplitude is considerably larger, > 10 mV (peak-to-peak), thus leading to the narrow line width. Third, the line width decreases with the reduction in phase fluctuations.[29] To verify this, we analyzed the time-resolved voltage signals (1 μs long in the current range of 0.1 to 0.8 mA) corresponding to the frequency-domain measurements in Figure 2a, b using the previously reported time-domain techniques.[31,32] The data show similar trends at a given current. A 200 ns long segment of the total time signal at I = 0.7 mA is presented in Figure 5 panels a and b for the in-plane field and the out-of-plane field cases, respectively, and the corresponding phase shifts are shown in Figure 5c. One can see that the phase fluctuation for the out-of-plane field (a change of 40 rad over a 1 μs time period) is obviously smaller than that for the in-plane field (a change of 125 rad over a 1 μs time period), which is partially responsible for the narrower line width in the case of the out-of-plane field. Therefore, the results confirm that in our system the application of the out-of-plane field can help reduce the phase noise and further narrow the line width.

CONCLUSIONS

In short, we have experimentally demonstrated the operation of STNOs having a planar free layer with perpendicular anisotropy. Microwave emissions having simultaneously a maximum measured power of 0.28 μW, a narrow line width of 25 MHz, a single oscillation mode, and high generation efficiency were achieved at small working currents and low static magnetic fields. These features make the presented STNOs promising candidates for nanoscale oscillators, which could replace transistor-based oscillators used in radio frequency integrated circuits (*e.g.*, local oscillators in radio frequency transmitters, receivers, and phase locked loops). Moreover, while the contribution of the perpendicular anisotropy is critical for the high-power microwave emission presented in this work, deeper understanding demands further detailed experimental and theoretical investigation. We believe our findings will stimulate such activities, resulting in a better understanding of large-amplitude dynamic magnetization phenomena and pave the way for developing practical high-power nanoscale oscillators.

METHODS

Sample Preparation. The continuous multilayer thin films with stacks of composition PtMn (15) /$Co_{70}Fe_{30}$ (2.3)/Ru (0.85)/$Co_{40}Fe_{40}B_{20}$ (2.4)/MgO (0.8)/$Co_{20}Fe_{60}B_{20}$ (wedge: 1.6−2.0) (thickness in nm) were deposited using a Singulus TIMARIS PVD system and annealed at 300 °C for 2.0 h in a magnetic field of 1 T. The films were subsequently patterned into ellipse-shaped pillars with different aspect ratios and sizes using electron-beam lithography and ion milling techniques. Details of the devices and their spin-transfer switching performance can be found in our previous work.[26]

Transport Measurements. We performed all transport measurements at room temperature by contacting the pillars *via* top and bottom electrodes through a high-bandwidth (40 GHz) probe, with a GMW projected field electromagnet[17] that allows us to control the field continuously in 3 dimensions (x, y, z). For the static measurements, a Keithley Instruments Source Meter was used. For the dynamic experiments similar to those in ref 14, a bias T was used to separate the dc current injection from the dynamic output signal, which was directly recorded by a 26 GHz spectrum analyzer, or a high speed real time oscilloscope with 6 GHz bandwidth and 20 G samples/s rate without amplifier as

shown in Figure 1a. For frequency-domain measurements, the spectra were taken with a resolution bandwidth (Δf) of 2 MHz. A baseline taken at $I = 0$ mA was subtracted from the measured spectral data. Note that the microwave emission is strongly dependent on the in-plane field direction β,[17,33,34] and we found that the microwave signals have large power and narrow line width at $\beta = 120°$. The results presented in this paper were obtained at $\beta = 120°$ and various out-of-plane angles φ as shown in Figure 1b.

The dynamic peak-to-peak resistance variations ΔR_{dyn}, plotted in Figure 4, are obtained from the spectra by calculating the area under the respective peaks, yielding the total rms power ΔV^2 similar to that in ref 10. Thus the resistance variation ΔR_{dyn} is given by

$$\Delta R_{dyn} = 2\sqrt{2}\Delta R_{rms} \quad \text{with} \quad \Delta R_{rms} = \frac{\Delta V_{gen}}{I},$$

$$\Delta V_{gen} = \left(\frac{Z_0 + R}{Z_0}\right)\Delta V$$

where Z_0 is the input impedance of the spectrum analyzer and R is the resistance of the MTJ nanopillar.

Conflict of Interest: The authors declare no competing financial interest.

Acknowledgment. We would like to thank A. Slavin, M. W. Keller, J. Zhao, P. Upadhyaya, Y.-J. Chen, G. Rowlands, K. H. Cheung, M. G. House, J. G. Alzate, and Y. Zhang for fruitful discussions. This work was supported by the DARPA STT-RAM program, the DARPA NV Logic program, and by the Nanoelectronics Research Initiative (NRI) through the Western Institute of Nanoelectronics (WIN).

Supporting Information Available: The effect of impedance mismatch, out-of-plane field angle dependence of STNOs performance, analysis of time-resolved microwave signals, in-plane field dependence of microwave signals and micromagnetic simulations. This material is available free of charge *via* the Internet at http://pubs.acs.org.

REFERENCES AND NOTES

1. Berger, L. Emission of Spin Waves by a Magnetic Multilayer Traversed by a Current. *Phys. Rev. B* **1996**, *54*, 9353–9358.
2. Slonczewski, J. C. Current-Driven Excitation of Magnetic Multilayers. *J. Magn. Magn. Mater.* **1996**, *159*, L1–L7.
3. Kiselev, S. I.; Sankey, J. C.; Krivorotov, I. N.; Emley, N. C.; Schoelkopf, R. J.; Buhrman, R. A.; Ralph, D. C. Microwave Oscillations of a Nanomagnet Driven by a Spin-Polarized Current. *Nature* **2003**, *425*, 380–383.
4. Rippard, W. H.; Pufall, M. R.; Kaka, S.; Russek, S. E.; Silva, T. J. Direct-Current Induced Dynamics in $Co_{90}Fe_{10}/Ni_{80}Fe_{20}$ Point Contacts. *Phys. Rev. Lett.* **2004**, *92*, 027201.
5. Kaka, S.; Rippard, W. H.; Pufall, M. R.; Russek, S. E.; Silva, T. J.; Katine, J. A. Mutual Phase-Locking of Microwave Spin Torque Nano-oscillators. *Nature* **2005**, *437*, 389–392.
6. Mancoff, F. B.; Rizzo, N. D.; Engel, B. N.; Tehrani, S. Phase-Locking in Double-Point-Contact Spin-Transfer Devices. *Nature* **2005**, *437*, 393–395.
7. Pribiag, V. S.; Krivorotov, I. N.; Fuchs, G. D.; Braganca, P. M.; Ozatay, O.; Sankey, J. C.; Ralph, D. C.; Buhrman, R. A. Magnetic Vortex Oscillator Driven by dc Spin-Polarized Current. *Nat. Phys.* **2007**, *3*, 498–503.
8. Ruotolo, A.; Cros, V.; Georges, B.; Dussaux, A.; Grollier, J.; Deranlot, C.; Guillemet, R.; Bouzehouane, K.; Fusil, S.; Fert, A. Phase-Locking of Magnetic Vortices Mediated by Antivortices. *Nat. Nanotechnol.* **2009**, *4*, 528–532.
9. Dussaux, A.; Georges, B.; Grollier, J.; Cros, V.; Khvalkovskiy, A. V.; Fukushima, A.; Konoto, M.; Kubota, H.; Yakushiji, K.; Yuasa, S.; *et al.* Large Microwave Generation from Current-Driven Magnetic Vortex Oscillators in Magnetic Tunnel Junctions. *Nat. Comm.* **2010**, *1*, 1006.
10. Houssameddine, D.; Ebels, U.; Delaët, B.; Rodmacq, B.; Firastrau, I.; Ponthenier, F.; Brunet, M.; Thirion, C.; Michel, J.-P.; Prejbeanu-Buda, L.; *et al.* Spin-Torque Oscillator using a Perpendicular Polarizer and a Planar Free Layer. *Nat. Mater.* **2007**, *6*, 447–453.
11. Slavin, A. Microwave Sources: Spin-Torque Oscillators Get in Phase. *Nat. Nanotechnol.* **2009**, *4*, 479–480.
12. Nazarov, A. V.; Olson, H. M.; Cho, H.; Nikolaev, K.; Gao, Z.; Stokes, S.; Pant, B. B. Spin Transfer Stimulated Microwave Emission in MgO Magnetic Tunnel Junctions. *Appl. Phys. Lett.* **2006**, *88*, 162504.
13. Houssamedine, D.; Florez, S. H.; Katine, J. A.; Michel, J.-P.; Ebels, U.; Mauri, D.; Ozatay, O.; Delaet, B.; Viala, B.; Folks, L.; *et al.* Spin Transfer Induced Coherent Microwave Emission with Large Power from Nanoscale MgO Tunnel Junctions. *Appl. Phys. Lett.* **2008**, *93*, 022505.
14. Deac, A.; Fukushima, A.; Kubota, H.; Maehara, H.; Suzuki, Y.; Yuasa, S.; Nagamine, Y.; Tsunekawa, K.; Djayaprawira, D. D.; Watanabe, N. Bias-Driven High-Power Microwave Emission from MgO-Based Tunnel Magnetoresistance Devices. *Nat. Phys.* **2008**, *4*, 803–809.
15. Georges, B.; Grollier, J.; Cros, V.; Fert, A.; Fukushima, A.; Kubota, H.; Yakushiji, K.; Yuasa, S.; Ando, K. Origin of the Spectral Linewidth in Nonlinear Spin-Transfer Oscillators Based on MgO Tunnel Junctions. *Phys. Rev. B* **2009**, *80*, 060404(R).
16. Masugata, Y.; Ishibashi, S.; Tomita, H.; Seki, T.; Nozaki, T.; Suzuki, Y.; Kubota, H.; Fukushima, A.; Yuasa, S. Spin-Torque Induced rf Oscillation in Magnetic Tunnel Junctions with an Fe-rich CoFeB Free Layer. *J. Phys.: Conf. Ser.* **2011**, *266*, 012098.
17. Zeng, Z. M.; Upadhyaya, P.; Khalili Amiri, P.; Cheung, K. H.; Katine, J. A.; Langer, J.; Wang, K. L.; Jiang, H. W. Enhancement of Microwave Emission in Magnetic Tunnel Junction Oscillators through In-Plane Field Orientation. *Appl. Phys. Lett.* **2011**, *99*, 032503.
18. Houssamedine, D.; Ebels, U.; Dieny, B.; Garello, K.; Michel, J.-P.; Delaet, B.; Viala, B.; Cyrille, M.-C.; Katine, J. A.; Mauri, D. Temporal Coherence of MgO Based Magnetic Tunnel Junction Spin Torque Oscillators. *Phys. Rev. Lett.* **2009**, *102*, 257202.
19. Devolder, T.; Bianchini, L.; Kim, Joo-Von; Crozat, P.; Chappert, C.; Cornelissen, S.; Op de Beeck, M.; Lagae, L. Auto-oscillation and Narrow Spectral Lines in Spin-Torque Oscillators Based on MgO Magnetic Tunnel Junctions. *J. Appl. Phys.* **2009**, *106*, 103921.
20. Krivorotov, I. N.; Berkov, D. V.; Gorn, N. L.; Emley, N. C.; Sankey, J. C.; Ralph, D. C.; Buhrman, R. A. Large-Amplitude Coherent Spin Waves Excited by Spin-Polarized Current in Nanoscale Spin Valves. *Phys. Rev. B* **2007**, *76*, 024418.
21. Slavin, A.; Tiberkevich, V. Nonlinear Auto-oscillator Theory of Microwave Generation by Spin-Polarized Current. *IEEE Trans. Magn.* **2009**, *45*, 1875–1918.
22. Zhang, S.; Levy, P. M.; Marley, A. C; Parkin, S. S. P. Quenching of Magnetoresistance by Hot Electrons in Magnetic Tunnel Junctions. *Phys. Rev. Lett.* **1997**, *79*, 3744–3747.
23. Sun, J. Z. Spin-Current Interaction with a Monodomain Magnetic Body: A Model Study. *Phys. Rev. B* **2000**, *62*, 570–578.
24. Liu, L.; Moriyama, T.; Ralph, D. C.; Buhrman, R. A. Reduction of the Spin-Torque Critical Current by Partially Canceling the Free Layer Demagnetization Field. *Appl. Phys. Lett.* **2009**, *94*, 122508.
25. Yakata, S.; Kubota, H.; Suzuki, Y.; Yakushiji, K.; Fukushima, A.; Yuasa, S.; Ando, K. Influence of Perpendicular Magnetic Anisotropy on Spin-Transfer Switching Current in CoFeB/MgO/CoFeB Magnetic Tunnel Junctions. *J. Appl. Phys.* **2009**, *105*, 07D131.
26. Khalili Amiri, P.; Zeng, Z. M.; Langer, J.; Zhao, H.; Rowlands, G.; Chen, Y.-J.; Krivorotov, I. N.; Wang, J.-P.; Jiang, H. W.; Katine, J. A.; *et al.* Switching Current Reduction using Perpendicular Anisotropy in CoFeB−MgO Magnetic Tunnel Junctions. *Appl. Phys. Lett.* **2011**, *98*, 112507.
27. Ikeda, S.; Miura, K.; Yamamoto, H.; Mizunuma, K.; Gan, H. D.; Endo, M.; Kanai, S.; Hayakawa, J.; Matsukura, F.; Ohno, H. A Perpendicular-Anisotropy CoFeB-MgO Magnetic Tunnel Junction. *Nat. Mater.* **2010**, *9*, 721–724.

28. Wada, T.; Yamane, T.; Seki, T.; Nozaki, T.; Suzuki, Y.; Kubota, H.; Fukushima, A.; Yuasa, S.; Maehara, H.; Nagamine, Y.; *et al*. Spin-Transfer-Torque-Induced rf Oscillation in CoFeB/MgO/CoFeB Magnetic Tunnel Junctions under a Perpendicular Magnetic Field. *Phys. Rev. B* **2010**, *81*, 104410.
29. Kim, J. V.; Tiberkevich, V. S.; Slavin, A. N. Generation Linewidth of an Auto-oscillator with a Nonlinear Frequency Shift: Spin-Torque Nano-oscillator. *Phys. Rev. Lett.* **2008**, *100*, 017207.
30. Krivorotov, I. N.; Emley, N. C.; Buhrman, R. A.; Ralph, D. C. Time-Domain Studies of Very-Large-Angle Magnetization Dynamics Excited by Spin Transfer Torques. *Phys. Rev. B* **2008**, *77*, 054440.
31. Bianchini, L.; Cornelissen, S.; Kim, Joo-Von; Devolder, T.; van Roy, W.; Lagae, L.; Chappert, C. Direct Experimental Measurement of Phase-Amplitude Coupling in Spin Torque Oscillators. *Appl. Phys. Lett.* **2010**, *97*, 032502.
32. Keller, M. W.; Kos, A. B.; Silva, T. J.; Rippard, W. H.; Pufall, M. R. Time Domain Measurement of Phase Noise in a Spin Torque Oscillator. *Appl. Phys. Lett.* **2010**, *94*, 193105.
33. Thadani, K. V.; Finocchio, G.; Li, Z.-P.; Ozatay, O.; Sankey, J. C.; Krivorotov, I. N.; Cui, Y.-T.; Buhrman, R. A.; Ralph, D. C. Strong Linewidth Variation for Spin-Torque Nano-Oscillators as a Function of In-Plane Magnetic Field Angle. *Phys. Rev. B* **2008**, *78*, 024409.
34. Mizushima, K.; Nagasawa, T.; Kudo, K.; Saito, Y.; Sato, R. Decrease of Nonlinearity and Linewidth Narrowing in Spin-Transfer Oscillators under the External Field Applied near the Hard Axis. *Appl. Phys. Lett.* **2009**, *94*, 152501.